10940–10952 *Nucleic Acids Research, 2020, Vol. 48, No. 19* *Published online 3 October 2020*
doi: 10.1093/nar/gkaa756

CK2 kinase-mediated PHF8 phosphorylation controls TopBP1 stability to regulate DNA replication

Haihua Feng[1,†], Jingchen Lu[1,2,†], Xiaotian Song[1], Angkana Thongkum[1], Fan Zhang[1], Lihong Lou[1], Ofer Reizes[3], Alexandru Almasan[1] and Zihua Gong[1,4,*]

[1]Department of Cancer Biology, Cleveland Clinic Lerner Research Institute, Cleveland, OH 44195, USA, [2]Department of Medical Oncology, Xiangya Hospital, Central South University, Changsha, China, [3]Department of Cardiovascular & Metabolic Sciences, Cleveland Clinic Lerner Research Institute, Cleveland, OH 44195, USA and [4]Case Comprehensive Cancer Center, Case Western Reserve University School of Medicine, Cleveland, OH 44106, USA

Received February 10, 2020; Revised August 31, 2020; Editorial Decision September 01, 2020; Accepted September 03, 2020

ABSTRACT

ATR functions as a master regulator of the DNA-damage response. ATR activation requires the ATR activator, topoisomerase IIβ-binding protein 1 (TopBP1). However, the underlying mechanism of TopBP1 regulation and how its regulation affects DNA replication remain unknown. Here, we report a specific interaction between TopBP1 and the histone demethylase PHF8. The TopBP1/PHF8 interaction is mediated by the BRCT 7+8 domain of TopBP1 and phosphorylation of PHF8 at Ser854. This interaction is cell-cycle regulated and phosphorylation-dependent. PHF8 is phosphorylated by CK2, which regulates binding of PHF8 to TopBP1. Importantly, PHF8 regulates TopBP1 protein level by preventing its ubiquitination and degradation mediated by the E3 ligase UBR5. Interestingly, PHF8pS854 is likely to contribute to regulation of TopBP1 stability and DNA replication checkpoint. Further, both TopBP1 and PHF8 are required for efficient replication fork restart. Together, these data identify PHF8 as a TopBP1-binding protein and provide mechanistic insight into how PHF8 regulates TopBP1 stability to maintain DNA replication.

INTRODUCTION

Genomic stability following DNA damage depends on the coordination of cell cycle checkpoint control and proper DNA repair. ATR (ataxia telangiectasia mutated- and Rad3-related) functions as a master regulator of the DNA damage response, especially during DNA replication. The ATR-activation process requires the ATR activator topoisomerase IIβ-binding protein 1 (TopBP1) (1,2). Human TopBP1 plays essential roles in DNA replication initiation, checkpoint signaling, and DNA repair and influences transcriptional control (3,4).

TopBP1 contains eight BRCA1 carboxyl-terminal (BRCT) phosphopeptide recognition motifs and an ATR-activating domain (AAD) (3,4). TopBP1 utilizes its BRCT motifs as scaffolds to modulate multiple cellular pathways (3,4). The AAD domain is sufficient to activate ATR *in vitro* and *in vivo* (5). Recent reports showed that ETAA1 is recruited directly by RPA and functions independently of the 911 complex and TopBP1 to activate ATR (6–8), indicating that TopBP1 and ETAA1 act in separate pathways to regulate ATR and maintain genome stability. The BRCT 1/2 domain of TopBP1 interacts with the phosphorylated RAD9 in the 9–1–1 complex and is required for ATR-mediated Chk1 activation, which then leads to cell cycle arrest and DNA damage repair (9,10). The BRCT 1/2 domain is also required for binding to Treslin (TICRR), which functions in DNA replication initiation (11,12). The fifth BRCT domain (BRCT5) of TopBP1 is required for its localization to DNA damage sites (13). Recently, we demonstrated that the BRCT5 domain is responsible for the interaction of TopBP1 with phosphorylated MDC1 and it is required for efficient Chk1 phosphorylation after replication stress (14). We and others also found that TopBP1 interacted with Bloom syndrome helicase (BLM) through its BRCT5 domain and has an unexpected role in suppressing sister chromatid exchange (15,16). The TopBP1/BLM interaction has been further confirmed by crystal structural analysis (17). As for the C-terminal tandem BRCT domains (the seventh and eighth BRCT repeats) in TopBP1, we reported that this region associates with BACH1, which is required for early replication checkpoint control (18). In addition, Liu *et al.* showed that this region of TopBP1 binds to phosphorylated ATR and enables TopBP1 to engage ATR-ATRIP and stimulate ATR kinase activity (19). Thus, TopBP1 acts as a signal

*To whom correspondence should be addressed. Tel: +1 216 445 9652; Email: gongz@ccf.org
†The authors wish it to be known that, in their opinion, the first two authors should be regarded as Joint First Authors.
The research work was done at Cleveland Clinic.

integrator that functions primarily in DNA replication and replication checkpoint control.

In this study, we report a specific interaction between TopBP1 and plant homeo domain finger protein 8 (PHF8). PHF8 contains two functional domains: an N-terminal plant homeodomain (PHD) finger recognizing lysine-methylated histones and mediating binding to nucleosomes at active gene promoters and a Jumonji C-domain (JmjC) domain catalyzing lysine demethylation (20–23). Here we provide evidence that phosphorylated PHF8 interacts with TopBP1 and controls its protein level to maintain genome stability.

MATERIALS AND METHODS

Cell Culture and Plasmids

HeLa, HEK 293T, MCF10A, MCF-7 and MDA-MB-231 cells were purchased from the American Type Culture Collection (ATCC) and cultured under conditions specified by the ATCC. *TopBP1*$^{LoxP/LoxP}$; MEF and *TopBP1*$^{LoxP/LoxP}$;*Cre*^{TM} MEF cells were generously provided by Dr Peter Mckinnon (St. Jude Children's Research Hospital, Memphis, TN, USA) (24). The PHF8 cDNA was cloned using the Gateway technology. All mutants were generated by site-directed mutagenesis and verified by DNA sequencing.

Antibodies

Rabbit polyclonal anti-TopBP1 antibody was described previously (14,15,18). Anti-PHF8 pS854 polyclonal antibody was raised against phospho-peptide CFKDAEYIYPpSerLESDDD and affinity purified. The following antibodies were used for Western blotting and immunoprecipitation: FLAG (F3165, Sigma), β-actin (A5441, Sigma), HA (PI26183, Thermo Fisher Scientific), Myc (sc-40, Santa Cruz), GST (sc-138, Santa Cruz), GAPDH (sc-47724, Santa Cruz), PCNA (sc-56, Santa Cruz), Chk1 (sc-56291, Santa Cruz), PHF8 (ab36068, Abcam), pChk1S345 (2348S, Cell Signaling Technology), CK2α (10992–1-AP, Proteintech), H3 (04–928, Millipore) and MBP (AB3596, Millipore).

Coimmunoprecipitation and western blotting

Cells were lysed on ice for 30 min with NETN buffer (20 mM Tris–HCl, pH 8.0, 100 mM NaCl, 1 mM EDTA, 0.5% Nonidet *P*-40) containing protease inhibitors. Cell lysates were collected after centrifugation and incubated with either protein A agarose beads coupled with anti-TopBP1 antibody overnight or streptavidin sepharose beads for 2 h at 4°C. The precipitates were then washed with NETN and boiled in 2× SDS loading buffer for 8 min. Samples were resolved by SDS-PAGE, transferred to PVDF membranes, and immunoblots were carried out with antibodies as indicated.

Tandem Affinity Purification

HEK 293T cells stably expressing SFB-TopBP1 BRCT7+8 and SFB-PHF8 were used for tandem affinity purification. Cells stably expressing SFB-TopBP1 BRCT7+8 and SFB-PHF8 were lysed with NETN buffer on ice for 20 min. After removal of cell debris by centrifugation, crude lysates were incubated with streptavidin sepharose beads for 1 h at 4°C. The bead-bound proteins were washed 3 times with NETN buffer and eluted twice with 2 mg/ml biotin for 1 h at 4°C. The eluates were combined and then incubated with streptavidin sepharose beads for 1 h at 4°C. The beads were washed three times with NETN buffer. The bead-bound proteins were separated by SDS-PAGE and visualized by Coomassie Blue staining. The eluted proteins were identified by mass spectrometry analysis, which was performed by the Taplin Biological Mass Spectrometry Facility (Harvard Medical School).

Cell synchronization and fluorescence-activated cell sorting

HeLa cells were treated with 2 mM thymidine for 19 h and released in fresh medium for 9 h. Thymidine (2 mM) was added again, and cells were incubated for another 9 h in order to arrest cells in G1 phase before releasing them again in fresh medium. Cells were collected at the indicated time points. For cell-cycle analysis, synchronized cells were washed twice with PBS, resuspended in 300 μl PBS, and fixed with the addition of 700 μl 100% ethanol. After storage at –20°C overnight, fixed cells were washed and incubated in sodium citrate buffer containing RNase A for 60 min and then stained with propidium iodide for 30 min. Then, cells were run on a FACScan System, and cell-cycle analysis was performed.

Pull-down assays using bacterially expressed fusion proteins

GST or MBP fusion proteins were expressed in *Escherichia coli* and purified. The purified fusion proteins were immobilized on glutathione sepharose 4B or amylose resin and incubated with lysates prepared from cells transiently transfected with plasmids encoding the indicated proteins. The samples were subjected to SDS-PAGE and analyzed by western blotting.

Recombinant protein production

The GST proteins expressed in *E. coli* were purified using glutathione sepharose 4B beads and eluted with glutathione buffer (20 mM L-gluthathione; 50 mM Tris–HCl, pH 9.0). The MBP proteins expressed in *E. coli* were purified by amylose resin and eluted with maltose buffer (10 mM maltose; 20 mM Tris–HCl, pH 7.4; 200 mM NaCl; 1 mM EDTA; 10 mM β-mercaptoethanol).

In vitro phosphorylation assay

Cell lysates or bacterially expressed proteins were incubated with CK2 kinase following the manufacturer's instructions (New England Biolabs, P6010). Briefly, 2 mg protein was incubated with 1× NEBuffer for Protein Kinases supplemented with 200 μM ATP, 2 μM Na_3VO_4, 1 μM NaF and 500 units of CK2 kinase at 30°C for 1 h. The reaction was stopped by adding 2× loading buffer and boiling at 97°C for 10 min.

CRISPR–Cas9 gene-editing approach to generate PHF8-knockout cells

Designs were chosen to target the PHF8 gene in the first few exons and were tested for obvious potential off-targets by bioinformatics analysis. Plasmids expressing short-guide RNAs (sgRNAs) were constructed by inserting a pair of annealed oligonucleotides encoding the corresponding sgRNA into the PX458 vector. MCF10A or MDA-MB-231 cells were transfected with PX458-based plasmid vectors expressing PHF8 sgRNA, the Cas9 nuclease, and the GFP protein. Cells were then sorted and seeded as single colonies in 96-well plates by fluorescence-activated cell sorting (FACS). After 2 weeks, clones were selected based on western blotting with PHF8 antibody. In addition, genomic DNA was extracted from cell lines arising from single clones. PCR reactions to amplify targeted loci were performed, and agarose gel electrophoresis was used to confirm the correct size of PCR products. PCR products were then cloned into the pCR2.1-TOPO vector and transformed into DH5α competent cells. Plasmid DNA was isolated from multiple colonies of each transformation and sequenced to ensure frameshift mutations in the targeted region.

The sequence information for sgRNAs used for PHF8 knockout (KO) cell generation is as follows:

PHF8_sgRNA1: GCACCGAGGCCATCTTCGCT
PHF8_sgRNA2: TGGCATTTGTTGGGCGGATC

Isolation of soluble and chromatin isolation

Cellular fractions were prepared as previously described (25). Briefly, cells were collected, washed with PBS, and lysed in hypotonic buffer A (10 mM HEPES [pH 7.9], 10 mM KCl, 1.5 mM $MgCl_2$, 0.34 M sucrose, 10% glycerol, 1 mM DTT, and protease inhibitors). Triton X-100 was added to 0.1%, the cells were incubated on ice for 10 min. After centrifugation (4 min, 1200 g, 4°C), the supernatant was collected as soluble fraction and the pellet was washed twice in buffer A and lysed for 30 min in buffer B (3 mM EDTA, 0.2 mM EGTA, 1 mM DTT and protease inhibitors) on ice. After centrifugation (4 min, 1700 g, 4°C), insoluble pellet was washed twice in buffer B. The final chromatin pellet was resuspended in buffer C (50 mM Tris–HCl [pH 8.0], 300 mM NaCl, 1% NP-40, 1 mM DTT and protease inhibitors) on ice for 10 min and sonicated twice for 10 s using a microtip at 30% amplitude. The supernatant was collected as chromatin fraction by high-speed centrifugation (15 min, 20 000 × g, 4°C).

DNA fiber analysis

The DNA fiber assay was conducted as previously described (26,27). Cells were treated with IdU and CIdU to obtain a final concentration of 25 and 250 μM, respectively. The treated cells were harvested with 0.25% trypsin-EDTA and resuspended in ice-cold PBS. Cells were lined on glass slides and lysed with lysis solution (0.2 M Tris–HCl pH 7.5, 0.5 mM EDTA, 0.5% SDS) before tilting the slide to allow the fibers to spread over the slide. The slides then were fixed with methanol:acetic acid (3:1) for 10 min before the DNA was denatured with 2.5 M HCl for 80 min, followed by washing with PBS and blocking with 5% BSA for 30 min. The slides were stained with primary antibody overnight at 4°C, washed with PBS, and incubated with secondary antibody for 2 h at room temperature. Slides were then washed with PBS, Prolong Gold anti-fade medium added and the slides were then coverslipped. Slides were imaged using Leica DM4 B microscope. Image analysis were analyzed with ImageJ. A minimum of 150 tracts was measured for each experiment to determine the percentage of stalled forks and the IdU:CIdU ratio. Three independent experiments were performed.

RESULTS

PHF8 Interacts with TopBP1

Proteins associated with TopBP1 BRCT domains appear to be important for TopBP1's functions (3,4,9,10,12,14,15,18). We generated stable cell lines expressing the triple (SFB)-tagged BRCT7+8 domain of TopBP1. These cells were then expanded and used for tandem affinity purification (TAP). Mass spectrometry (MS) analysis revealed that, in addition to BACH1 (18), PHF8 was also associated with TopBP1 (Figure 1A). PHF8, a histone H4K20/H3K9 demethylase, plays key roles in cell cycle regulation, rDNA transcription and zebrafish brain and craniofacial development (20–23). Furthermore, we repeatedly identified TopBP1 as a major PHF8-associated protein through TAP, using lysates derived from HEK 293T cell lines that stably express SFB-tagged human PHF8 (Figure 1B). Using bacterially expressed and purified proteins, we further confirmed that the TopBP1 BRCT 7+8 domain binds to PHF8 (Figure 1C). Moreover, we confirmed the binding of TopBP1 to PHF8 through endogenous co-immunoprecipitation experiments, suggesting that these two proteins indeed associate with each other *in vivo* (Figure 1D). Furthermore, we isolated soluble and chromatin fractions and performed immunoprecipitations. As shown in Supplemental Figure S6, the TopBP1-PHF8 interaction exists in both the soluble fraction and chromatin fraction, but it is more prevalent in the chromatin fraction.

TopBP1 Interacts with PHF8 through residue R1314

Next, we sought to define the PHF8 binding region(s) on TopBP1. A series of TopBP1 BRCT deletion mutants were described previously (18) (Figure 2A). By performing a co-immunoprecipitation experiment, we observed that deletions of either the seventh or eighth BRCT domain of TopBP1 led to a striking decrease in TopBP1/PHF8 interaction (Figure 2B). Furthermore, deletion of both BRCT7 and BRCT8 completely abolished the interaction, indicating that the very C-terminal tandem BRCT domains of TopBP1 were important for its binding to PHF8. In addition, we exploited a recently identified small molecule, calcein-AM, that binds to BRCT domains 7 and 8 (28), and observed that the TopBP1-PHF8 interaction was drastically decreased (Figure 2C), suggesting that calcein-AM binding to BRCT7 and BRCT8 blocks its interaction with PHF8. We have already solved the structures of the TopBP1 BRCT7 and BRCT8 domains and its complex with BACH1 (29). Mutation of residues S1273/R1280/R1314 within the BRCT7 and BRCT8 domains abolished the TopBP1/BACH1 interaction (29).

A

Proteins associated with TopBP1 BRCT7/8

Protein	Number of Peptides
TopBP1	16
BRIP1	14
BRCA1	13
PHF8	6
SET	4
...	

B

Proteins associated with PHF8

Protein	Number of Peptides
PHF8	46
Cyclin A2	9
TopBP1	8
CDK2	7
SMC2	4
...	

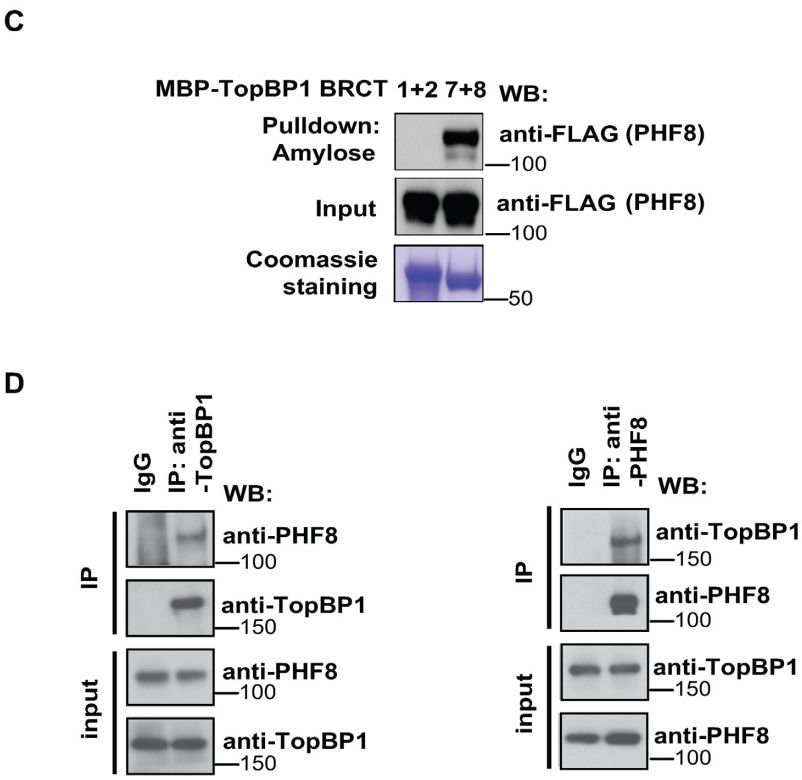

Figure 1. PHF8 interacts with TopBP1. (**A**) A List of TopBP1 BRCT7+8-associated proteins identified by mass spectrometric analysis. (**B**) A List of PHF8-associated proteins identified by mass spectrometric analysis. (**C**) TopBP1 specifically binds to PHF8. Beads coated with bacterially expressed MBP fusion of BRCT7+8 or BRCT1+2 of TopBP1 were incubated with cell lysates containing exogenously expressed SFB-tagged PHF8. Immunoblotting experiments were carried out using the indicated antibodies. (**D**) Endogenous interaction between TopBP1 and PHF8. HEK 293T cell lysates were prepared and immunoprecipitated with TopBP1 or PHF8 antibody. Immunoprecipitates were blotted using antibodies, as indicated.

We wanted to further investigate the binding affinity of TopBP1/PHF8 by using these TopBP1 mutation sites. As shown in Figure 2D, the R1314Q mutant of TopBP1 notably affected the TopBP1/PHF8 interaction, suggesting that the Arg1314 residue of TopBP1 is the major site involved in the TopBP1/PHF8 interaction.

Residue Ser854 of PHF8 is required for its interaction with TopBP1

To further characterize this interaction, a series of PHF8 deletion mutants were constructed to define the TopBP1 binding region(s) on PHF8 (Figure 3A) and mapped the minimal TopBP1 binding region to residues 801–901 of PHF8 (Figure 3B, C). Because the BRCT domain is a phosphoprotein binding domain, we assumed that BRCT7 and BRCT8 domains of TopBP1 might bind specifically to phosphorylated PHF8. To determine whether the interaction between TopBP1 and PHF8 is phosphorylation-dependent, we mutated all potential phosphorylation sites located within PHF8 residues 801–901. As shown in Figure 3D, mutation of both the Ser854 and Ser857 sites greatly reduced the TopBP1–PHF8 interaction. In addition, the Ser854 mutation alone behaved like the Ser854 and Ser857 double mutation (Figure 3E), which suggests that

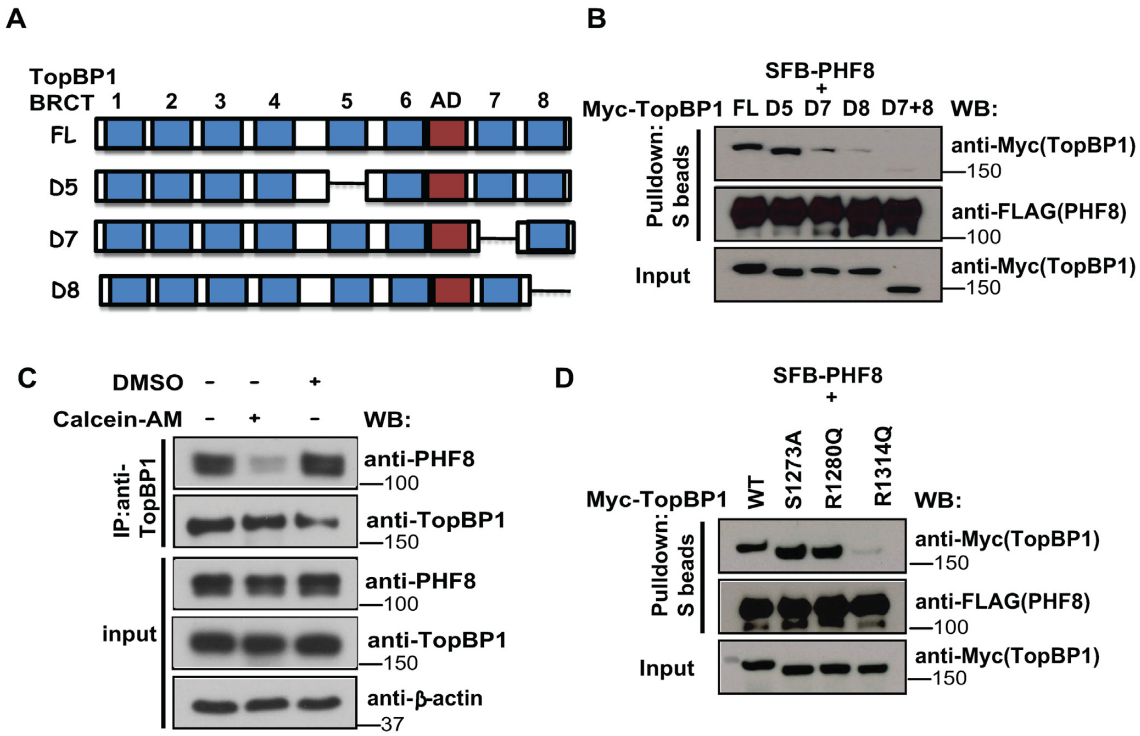

Figure 2. TopBP1 Interacts with PHF8 through residue R1314 of TopBP1. (**A**) Schematic presentation of WT and deletion mutants of TopBP1 used in this study. (**B**) The BRCT7+8 domain of TopBP1 is required for TopBP1-PHF8 interaction. HEK 293T cells were transfected with plasmids encoding SFB-tagged PHF8 along with plasmids encoding WT and deletion mutants of Myc-tagged TopBP1. Precipitation reactions were conducted with S beads and subjected to western blotting with the indicated antibodies. (**C**) Endogenous TopBP1 interaction with PHF8 decreased after calcein-AM treatment. HeLa cells were treated with calcein-AM (2.5 μM) or DMSO for 5 h before harvest. Control and anti-TopBP1 immunoprecipitates were immunoblotted with the indicated antibodies. (**D**) The R1314Q mutant of TopBP1 reduced the interaction with PHF8. HEK 293T cells were transfected with plasmids encoding SFB-tagged PHF8 along with plasmids encoding the S1273A, R1280Q or R1314Q mutants of Myc-tagged TopBP1. Immunoprecipitation reactions were conducted with S beads and subjected to western blotting with the indicated antibodies.

the Ser854 site is the major phosphorylation site involved in the TopBP1-PHF8 interaction. Indeed, the Ser854 residue of human PHF8 is conserved in other species, suggesting that this residue may be important for PHF8 function (Figure 3F). We generated a phospho-specific antibody raised against a peptide containing PHF8 phospho-Ser854. This antibody specifically recognized wild-type (WT) PHF8 but failed to recognize the S854A mutant (Figure 3G and Supplemental Figure S1).

To further confirm that the Ser854 phosphorylation site on PHF8 is required for its interaction with TopBP1, we synthesized phosphorylated and un-phosphorylated Ser854 peptides as well as phosphorylated Ser857 to perform pull-down experiments. As a result, both overexpressed TopBP1 and endogenous TopBP1 could be pulled down by the phosphorylated Ser854 peptide of PHF8 but not by the control un-phosphorylated peptide or phosphorylated Ser857 peptide (Supplemental Figure S2A-2B). Moreover, we performed a peptide competition assay. Only the phosphorylated PHF8 peptide, but not the unphosphorylated control peptide, competed with endogenous PHF8 for binding to the tandem BRCT7+8 domains of TopBP1 (Supplemental Figure S2C). In addition, we observed that the phosphorylated PHF8 peptide could disrupt the TopBP1/PHF8 interaction, whereas the un-phosphorylated peptide failed to do it (Supplemental Figure S2D), further confirming that TopBP1 binds selectively to the phosphorylated Ser854 site of PHF8.

Interaction between TopBP1 and PHF8 is cell-cycle and phosphorylation-dependent

Because TopBP1 functions mainly in the S and G2 phases, we determined whether its binding with PHF8 is cell cycle-dependent. As shown in Figure 4A, the PHF8-TopBP1 interaction reached a maximum in S phase. Altogether, these data indicate that the interaction between TopBP1 and PHF8 is dissociated following replication stress and is cell cycle-dependent. Importantly, phosphorylation of PHF8 at Ser854 was significantly enriched during S phase, an event that appears to correlate with its interaction with TopBP1 (Figure 4B) and indicates that Ser854 of PHF8 is indeed phosphorylated *in vivo* and this phosphorylation is cell cycle regulated. The BRCT domain is a phosphoprotein-binding domain (30,31). To determine whether the interaction between TopBP1 and PHF8 is phosphorylation-dependent, we treated cell lysates with λ protein phosphatase in a MBP pull-down assay. The interaction between MBP-TopBP1-BRCT7+8 and endogenous PHF8 decreased after treatment with λ protein phosphatase, suggesting that the interaction between TopBP1 and PHF8 is phosphorylation-dependent (Figure 4C). To further confirm that the PHF8

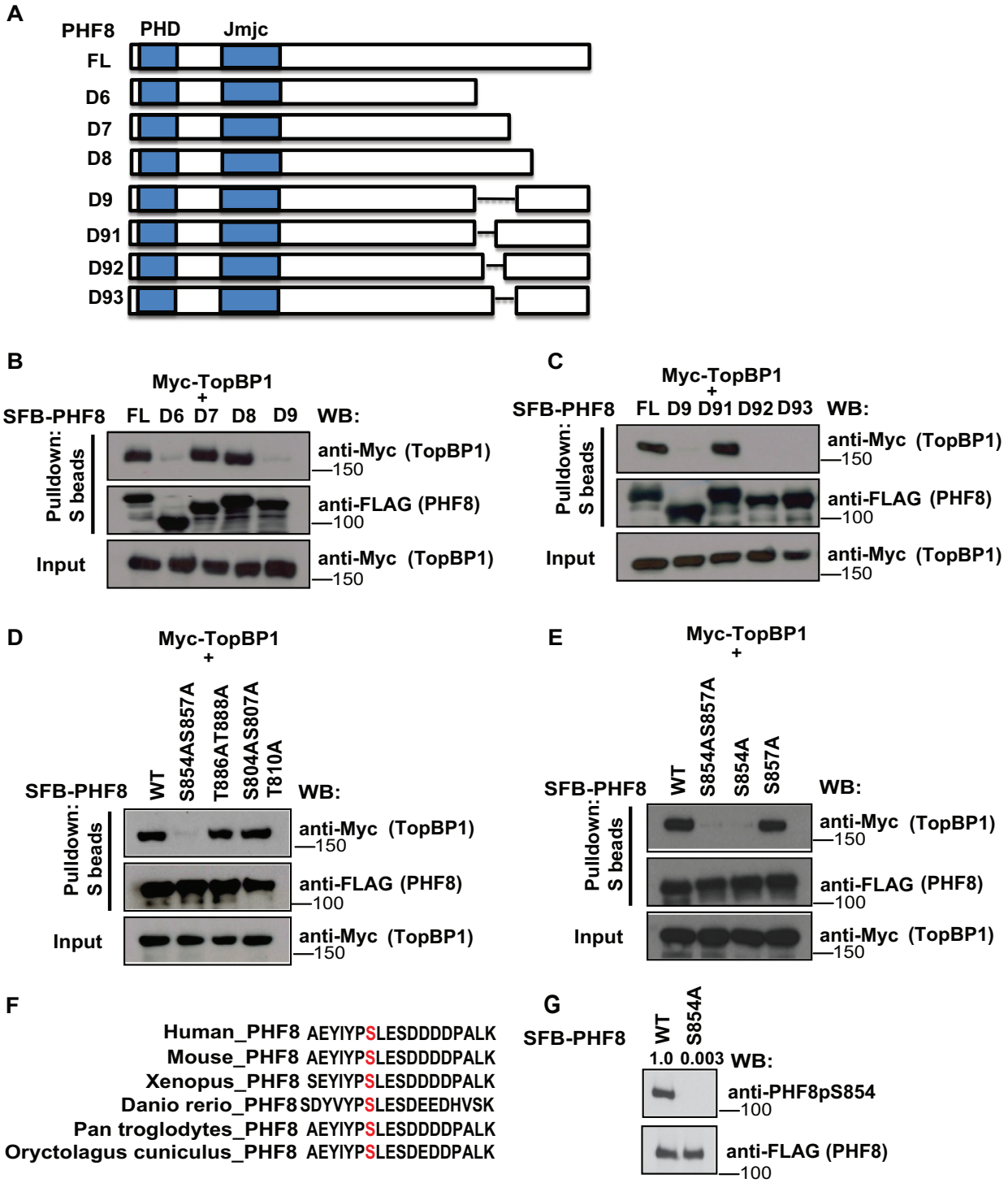

Figure 3. The Ser854 residue of PHF8 is required for its interaction with TopBP1. (**A**) Schematic presentation of WT and deletion mutants of PHF8 used in this study. (**B**, **C**) The C-terminal region of PHF8 is responsible for its interaction with TopBP1. HEK 293T cells were transfected with plasmids encoding SFB-tagged PHF8 WT and deletion mutants along with Myc-tagged TopBP1. Immunoprecipitation reactions were conducted with S beads and subjected to western blotting with the indicated antibodies. (**D**) The S854AS821A mutant of PHF8 reduced the interaction with TopBP1. HEK 293T cells were co-transfected with plasmids encoding Myc-tagged TopBP1 along with plasmids encoding SFB-tagged PHF8 WT and potential phospho-mutants. Immunoprecipitation reactions were conducted with S beads and subjected to western blotting with the indicated antibodies. (**E**) Ser854 of PHF8 is required for its interaction with TopBP1. HEK 293T cells were co-transfected with plasmids encoding Myc-tagged TopBP1 along with plasmids encoding SFB-tagged PHF8 WT and Ser854ASer857A, Ser854A, and Ser857A mutants. Immunoprecipitation reactions were conducted with S beads and subjected to western blotting with the indicated antibodies. (**F**) Alignment of the potential phospho-motif on PHF8 among species. (**G**) Recognition of PHF8 Ser854 by the phospho-Ser854 antibody. HEK 293T cells were transfected with plasmids encoding SFB-tagged PHF8 WT and Ser854A mutant. Immunoblotting experiments were performed using an antibody against PHF8 phosphorylated at S854.

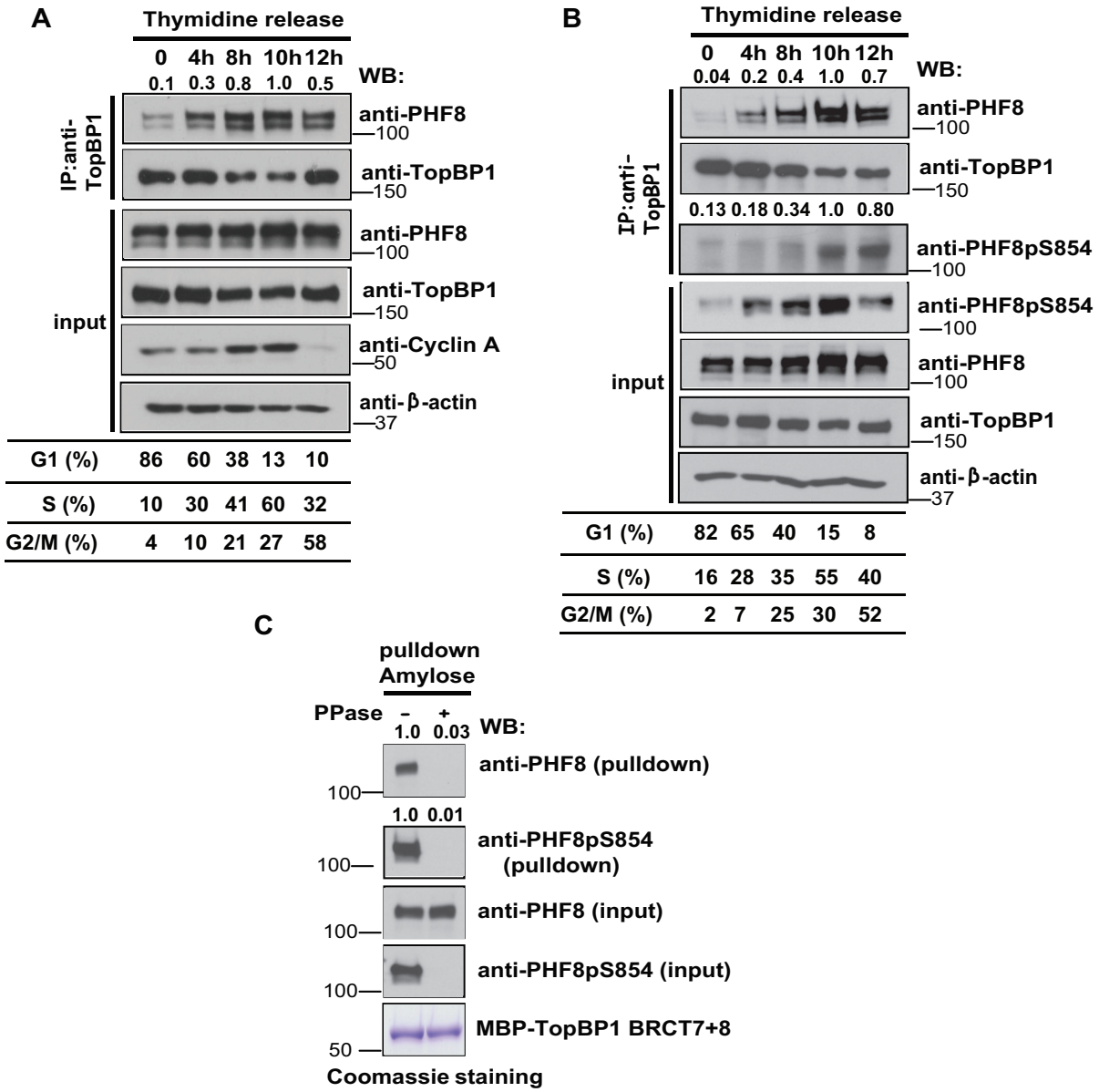

Figure 4. Interaction between TopBP1 and PHF8 is cell-cycle and phosphorylation dependent. (**A**) The interaction between TopBP1 and PHF8 is cell-cycle dependent. HeLa cells were synchronized by double thymidine block, released in fresh medium without thymidine, and collected at the indicated time points. Cell lysates were prepared, and immunoprecipitation and immunoblotting experiments were performed with the indicated antibodies. Samples were taken at the indicated time points and analyzed by fluorescence-activated cell sorting. (**B**) Phosphorylation of PHF8 at the S854 site is cell-cycle regulated. HeLa cells were synchronized by double thymidine block, and then released in fresh medium without thymidine and harvested at the indicated time points. Cell lysates were prepared, and immunoblotting experiments were performed using antibodies as indicated. Samples were taken at the indicated time points and analyzed by fluorescence-activated cell sorting. (**C**) TopBP1–PHF8 interaction is phosphorylation dependent. HEK-293T cells were lysed with NTEN buffer. Beads coated with bacterially expressed MBP-TopBP1 BRCT7+8 fusion protein were incubated with clear cell lysates that were mock treated or treated with λ protein phosphatase. Immunoblotting experiments were carried out with the indicated antibodies.

Ser854 phosphorylation site is required for its interaction with TopBP1, λ phosphatase treatment markedly decreased the signal detected by western blotting with this phospho-specific antibody, indicating that PHF8 Ser854 is indeed phosphorylated *in vivo*, and this S phase-specific phosphorylation of Ser854 is required for TopBP1-PHF8 interaction (Figure 4C). Collectively, these data suggest that the interaction between PHF8 and TopBP1 was cell-cycle and phosphorylation-dependent and phosphorylation of PHF8 at Ser854 is essential for their interaction.

CK2 kinase phosphorylates PHF8 on Ser854

To further explore which kinase is responsible for PHF8 phosphorylation at the Ser854 site, we found that this site (Ser854) fits well with the consensus motif (SXE/D, SXXE/D) that is phosphorylated by the CK2 kinase (Figure 5A). To test whether CK2 phosphorylates PHF8 on Ser854, we performed an *in vitro* phosphorylation assay using a bacterially expressed and purified MBP- or GST-fused PHF8 fragment containing Ser854 (760–954aa). Ser854

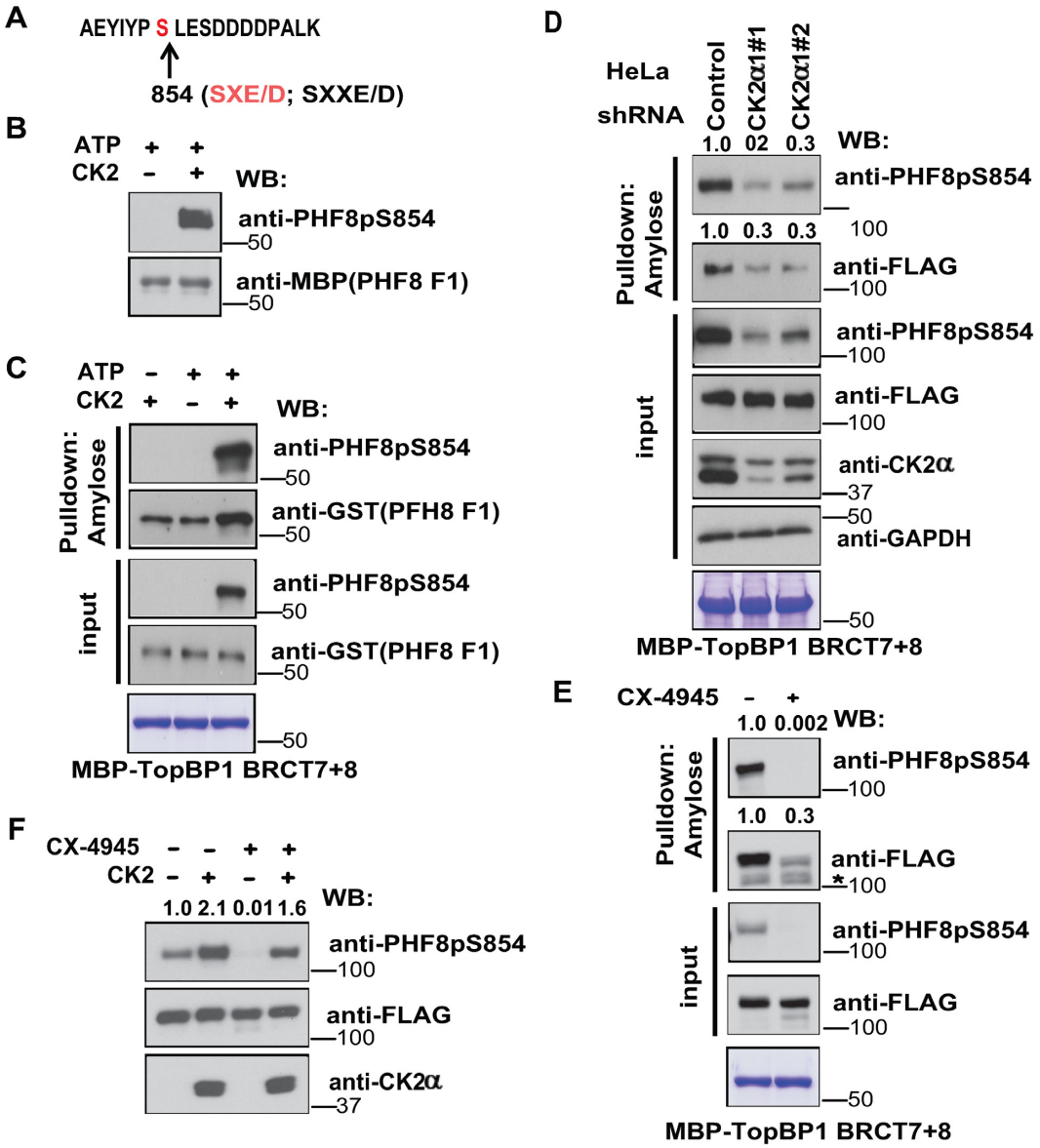

Figure 5. The CK2 kinase is responsible for PHF8 phosphorylation at Ser854. (**A**) PHF8 has the consensus sequence for CK2 kinase. (**B**) CK2 kinase phosphorylates PHF8 at Ser854 *in vitro*. Bacterially expressed and purified MBP-PHF8 fragment F1 (760–954aa) fusion proteins were incubated with or without bacterially expressed CK2. Immunoblotting experiments were performed using antibodies as indicated. (**C**) Phosphorylation of PHF8 by CK2 kinase increases its binding to TopBP1. Bacterially expressed and purified GST - PHF8 fragment F1 (760–954aa) fusion proteins were incubated with or without bacterially expressed CK2. Then beads coated with bacterially expressed MBP-TopBP1 BRCT7+8 fusion protein were added to the reaction and incubated. Beads were washed and boiled, and then subjected to western blotting using the indicated antibodies. (**D**) CK2 phosphorylates PHF8 at Ser854 *in vivo*. CK2α-stable knockdown (KD) Hela and HEK 293T cells were generated with CK2α shRNA lentivirus, then transfected with a plasmid encoding SFB-tagged PHF8. Beads coated with bacterially expressed MBP-TopBP1 BRCT7+8 fusion protein were incubated with cell lysates. Immunoblotting experiments were carried out using indicated antibodies. (**E**) The CK2 inhibitor CX-4945 inhibits PHF8 phosphorylation at Ser854. HEK 293T cells were transfected with a plasmid encoding SFB-tagged PHF8 and then incubated with or without CX-4945 (10 μM) for 24 h. Beads coated with bacterially expressed MBP-TopBP1 BRCT7+8 fusion protein were incubated with cell lysates. Immunoblotting experiments were carried out using indicated antibodies. * non-specific band. (**F**) CX-4945 inhibits CK2-mediated PHF8 phosphorylation at Ser854. HEK 293T cells were transfected with a plasmid encoding SFB-tagged PHF8 and then incubated with or without CX-4945 (10 μM) for 24 h. Cells were lysed with NTEN buffer. Clear cell lysates were incubated with streptavidin beads. Then the streptavidin beads were eluted with 2 mg/ml biotin in NTEN buffer. The eluates were further incubated with or without bacterially expressed CK2. Immunoblotting experiments were carried out with the indicated antibodies.

phosphorylation on PHF8 was detected in an ATP- and CK2-dependent manner (Figure 5B and C). Moreover, the binding of the GST-PHF8 fragment to MBP-TopBP1 BRCT7+8 increased in a phosphorylation-dependent manner (Figure 5C). To determine whether CK2 phosphorylates PHF8 on Ser854 *in vivo*, we examined the status of PHF8 phosphorylation on Ser854 when SFB-PHF8 was overexpressed in CK2α stably depleted HeLa cells. As shown in Figure 5D and Supplemental Figure S3, CK2α knockdown led to a significant decrease in PHF8 phosphorylation on Ser854. Next, we tested whether phosphorylation of PHF8 on Ser854 could be inhibited *in vitro* and *in vivo* by a highly specific inhibitor of CK2, CX-4945. After treatment with CX-4945, PHF8 phosphorylation on Ser854 was abolished in HEK 293T cells overexpressing SFB-PHF8. In addition, the binding of SFB-PHF8 or PHF8pS854 to TopBP1 BRCT7+8 strongly decreased in the presence of CX-4945 (Figure 5E). Furthermore, CK2-mediated PHF8 phosphorylation on Ser854 was inhibited by treatment with CX-4945, and the phosphorylation could be recovered by incubation with bacterially expressed CK2 kinase (Figure 5F). Together, these results demonstrate that CK2 phosphorylates PHF8 on Ser854, which is critical for the TopBP1-PHF8 interaction.

PHF8 regulates the TopBP1 protein level through UBR5-mediated ubiquitination

Given that TopBP1 interacts with PHF8, we explored the functional significance of this interaction. We observed that knockdown of PHF8 led to a strong decrease in TopBP1 protein level in both breast cancer MCF-7 and MDA-MB-231 cells (Figure 6A), suggesting that PHF8 regulates the protein level of TopBP1. Because a major function of TopBP1 is to regulate the replication checkpoint, we asked whether PHF8 has a similar function in checkpoint control. Indeed, knockdown of PHF8 inhibited hydroxyurea (HU)-induced Chk1 phosphorylation (Figure 6A).

To better understand how PHF8 regulates TopBP1 expression in the cell, we established MCF10A-derived PHF8-KO cells and treated them with the proteasome inhibitor MG132. We found that TopBP1 expression was restored (Figure 6B), suggesting that TopBP1 protein levels decrease through proteasomal degradation. It has been shown that the E3 ligase UBR5 (also named EDD1) promotes ubiquitination of TopBP1 (32). UBR5 contains two conserved domains, a HECT domain that is likely an E3 ubiquitin ligase and a PABC domain that is a protein-protein interaction domain. Expression of WT UBR5 led to reduced TopBP1 protein, a change that was completely reversed by the proteasome inhibitor MG132, whereas the UBR5ΔHECT deletion mutant did not affect TopBP1 protein level (Figure 6C), indicating that E3 ligase UBR5 is required for TopBP1 ubiquitination and degradation through its HECT domain. We also performed cycloheximide (CHX)) treatment experiments and showed that the half-life of TopBP1 with WT UBR5 was significantly shorter than that of TopBP1 with UBR5-ΔHECT, again supporting the idea that UBR5 mediated TopBP1 ubiquitination and degradation through its HECT domain (Figure 6D). To address how PHF8 regulates the UBR5-mediated degradation of TopBP1, we showed that depletion of UBR5 restored TopBP1 protein level in PHF8 KO cells (Figure 6E). Moreover, the CHX-chase method was performed to measure TopBP1 protein stability in the presence of WT and S854A mutant of PHF8. WT PHF8, but not the Ser854A mutant of PHF8, stabilizes the TopBP1 protein (Supplemental Figure S4), suggesting that PHF8 binding to TopBP1 may protect TopBP1 from degradation by UBR5. Next, we sought to identify ubiquitination sites on TopBP1. As shown in Figure 6F, only the N-terminus of TopBP1 was ubiquitinated by UBR5. To further map the ubiquitination sites, we will generate a series of truncation and deletion mutants, to identify the lysine residue(s) responsible for TopBP1 ubiquitination by UBR5. Altogether, PHF8 loss destabilizes TopBP1 protein level through UBR5-mediated TopBP1 ubiquitination and degradation.

The PHF8–TopBP1 interaction is involved in DNA replication

Because the level of TopBP1 protein markedly decreased with loss of PHF8 (Figure 6A and B) and PHF8 phosphorylation at Ser854 is critical for its interaction with TopBP1, we next investigated how PHF8 phosphorylation affects the TopBP1 protein level in PHF8-KO cells. Indeed, expression of WT PHF8, but not the S854A mutant of PHF8, restored the TopBP1 protein level in PHF8 KO cells (Figure 7A), indicating that the phosphorylation-dependent PHF8–TopBP1 interaction is required for TopBP1 expression. As shown in Figure 7A, downregulation of PHF8 inhibited APH-induced Chk1 phosphorylation. The expression of WT PHF8 fully restored Chk1 activation. However, the S854A mutant, which does not interact with TopBP1, failed to rescue Chk1 activation following APH treatment (Figure 7A). In addition, when we overexpressed TopBP1 in PHF8 KO cells, Chk1 activation was rescued in these cells (Supplemental Figure S5), indicating that PHF8's effect on DNA replication is at least partially through TopBP1.

To understand whether TopBP1 and PHF8 participate in replication fork progression, we used a DNA fiber assay to measure stalled replication forks and replication fork restart (Figure 7B). The DNA fiber assay allows for the labelling of actively progressing replication forks *in vivo* and the sequential incorporation of the two different halogenated nucleotides, IdU and CldU, into the nascent DNA strands to provide information about replication directionality (26,27). To monitor the natural dynamics of replication forks, we performed a DNA fiber assay in $TopBP1^{LoxP/LoxP};Cre^{TM}$ MEF cells (24). As shown in Figure 7C, 4-hydroxytamoxifen (4-OHT) effectively depleted TopBP1 in $TopBP1^{LoxP/LoxP};Cre^{TM}$ MEFs. In $TopBP1^{LoxP/LoxP}$(4-OHT) cells, the majority of forks resumed DNA synthesis, as manifested by red and green tracks (Figure 7B). In contrast, $TopBP1^{LoxP/LoxP};Cre^{TM}$ MEFs cells treated with 4-OHT exhibited a markedly increased frequency of stalled forks (red tracks only) and decreased frequency of restarted forks (IdU/CIdU), as summarized in Figure 7D. The DNA fiber assay revealed that the frequency of stalled forks increased and restart decreased in MCF10A-derived PHF8-KO cells (Figure 7E), suggesting that loss of PHF8 caused defects in replication

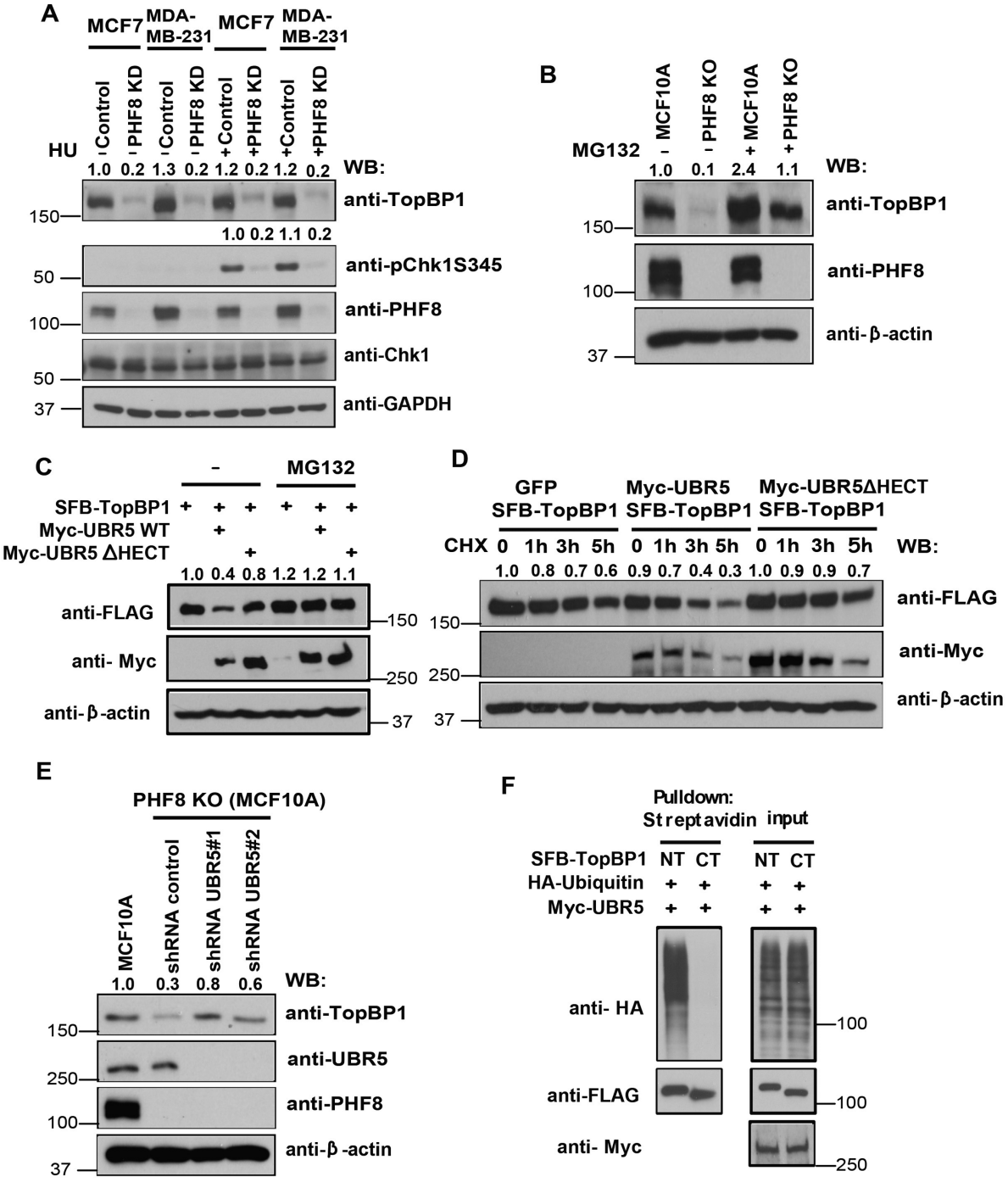

Figure 6. PHF8 regulates the TopBP1 protein level through UBR5-mediated ubiquitination. (**A**) TopBP1 protein level decreased in PHF8 KD cells. MCF-7/MCF-7 PHF8 KD and MDA-MB-231/MDA-MB-231 PHF8 KD cells were treated with HU (10 mM) for 1 h. Cells were harvested and immunoblotted with the indicated antibodies. (**B**) TopBP1 was degraded *via* a proteasome-mediated pathway in PHF8 KO cells. MCF10A-derived PHF8 KO cells were treated with 20 μM MG132 for 6 h. Cell lysates were subjected to western blotting with the indicated antibodies. (**C**) The HECT domain of UBR5 is required for TopBP1 degradation. HEK 293T cells were transfected with constructs encoding SFB-TopBP1 together with vector alone or constructs encoding Myc-tagged WT UBR5 or the UBR5ΔHECT mutant. At 24 h after transfection, cells were treated with the proteasome inhibitor MG132 (20 μM in DMSO), for 4 h. Cell lysates were examined by western blotting using the indicated antibodies. (**D**) The half-life of SFB-TopBP1 with Myc-UBR5 was shorter than that of SFB-TopBP1 with Myc-UBR5-ΔHECT. HEK 293T cells were transfected with constructs encoding SFB-tagged TopBP1 along with constructs encoding Myc-UBR5 or Myc-UBR5-ΔHECT. After treatment with cycloheximide (CHX, 10 μg/ml), cells were harvested at the indicated times and immediately lysed with 2x Laemmli buffer. The lysates were immunoblotted with the indicated antibodies. (**E**) Depletion of UBR5 restores TopBP1 expression in PHF8 KO cells. PHF8 KO cells were infected with control (CTR) shRNA, UBR5 shRNA#1 and UBR5 shRNA#2. Cell lysates were immunoblotted with the indicated antibodies. (**F**) The TopBP1 N-terminus is ubiquitinated by the E3 ligase, UBR5. HEK 293T cells were transfected with constructs encoding HA-ubiquitin, and Myc-UBR5 along with constructs encoding the SFB-TopBP1 N-terminus (1 aa–810 aa) or C-terminus (785 aa–1522 aa). Cell lysates were prepared and precipitated with streptavidin sepharose beads and subjected to western blotting with the indicated antibodies.

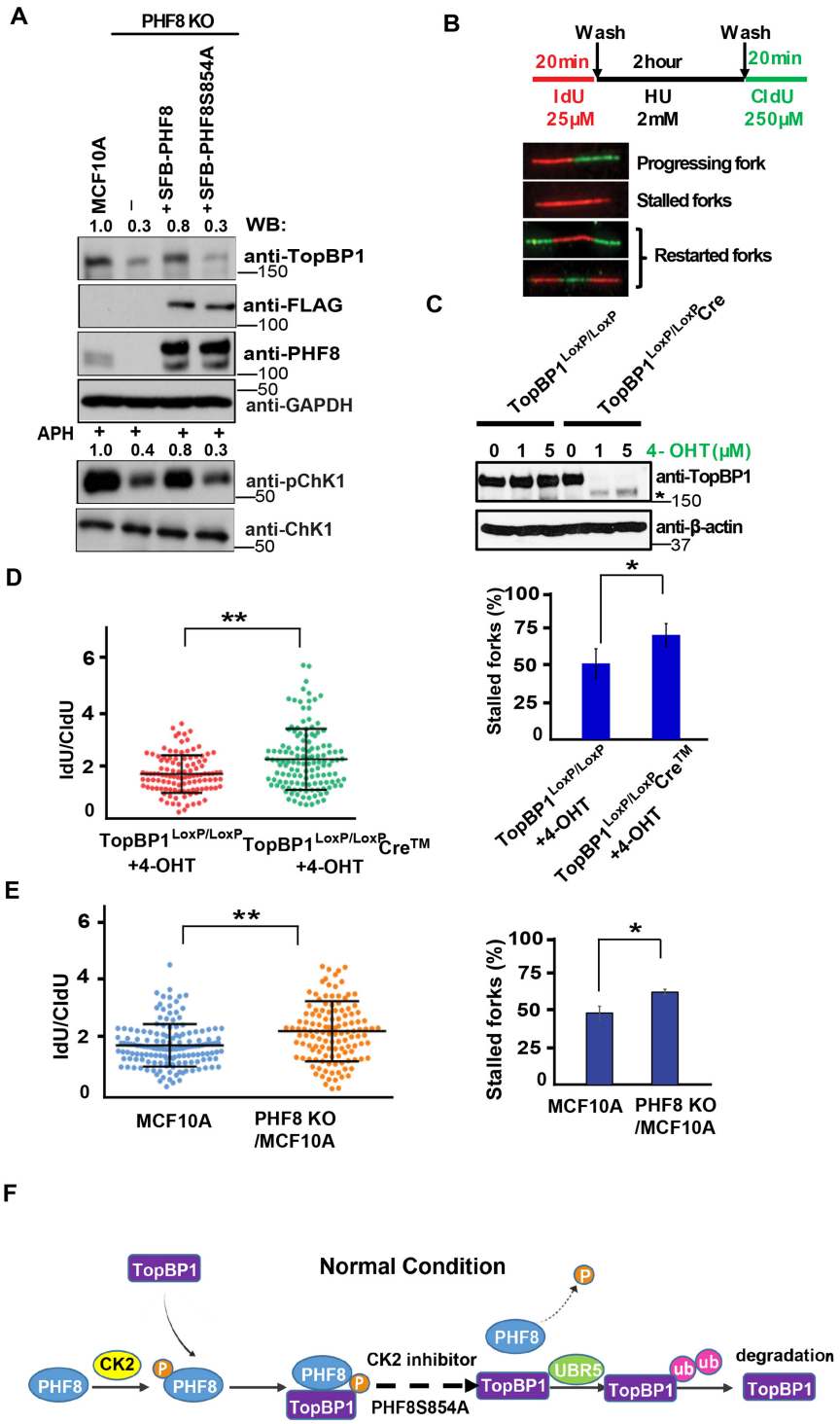

Figure 7. The PHF8-TopBP1 interaction is involved in DNA replication. (**A**) The PHF8-TopBP1 interaction is required for TopBP1 protein stability and DNA replication checkpoint activation. MCF10A and its derived PHF8 KO cells were reconstituted with WT or the S854A mutant of SFB-PHF8. Cells were treated with or without aphidicolin (APH, 20 μM) for 1 h. Cells were lysed with NTEN buffer and immunoblotted with the indicated antibodies. (**B**) Schematic of different replication events that can be studied by DNA fiber analysis and a representative image of the DNA fiber tracks are shown. (**C**) TopBP1 is depleted in $TopBP1^{LoxP/LoxP};Cre^{TM}$ MEF after 4-OHT administration. * non-specific band. (**D, E**) Loss of PHF8 caused defects in replication fork restart in response to HU treatment. Quantification of the restarted forks (IdU/CIdU) and stalled forks (%) by DNA fiber analysis in $TopBP1^{LoxP/LoxP}$ MEF and $TopBP1^{LoxP/LoxP};Cre^{TM}$ MEF inducible with 4-OHT (D); MCF10A and MCF10A-derived PHF8 KO cells (E). Briefly, cells were treated with IdU, HU, and CIdU, as described in *Materials and Methods*. The ratio of IdU/CIdU tract length from three independent experiments was plotted as mean ± s.d. Data for stalled replication forks (%) are calculated using mean ± s.d. of three independent experiments. WT and KO groups were compared using a paired *t*-test. * $P < 0.01$, ** $P < 0.001$. (**F**) A proposed model representing the regulation of TopBP1 by PHF8 under normal condition. Under normal condition, PHF8 regulates the protein level of TopBP1. E3 ligase UBR5 mediates TopBP1 ubiquitination and degradation in the soluble cellular fractions. Our data provided novel insights into the regulation of protein level of TopBP1 under normal conditions.

fork restart in response to HU treatment. Similar results were obtained in PHF8 KO of MDA-MB-231 breast cancer cells with PHF8 KO (Supplemental Figure S7). Together, these results indicate that TopBP1 and PHF8 promote the restart of the replication fork after replication stress.

DISCUSSION

Human TopBP1 is a key scaffold protein that can interact with many other proteins and play essential roles in a diverse range of cellular pathways, including DNA replication initiation, checkpoint signaling, DNA repair, and transcriptional control. Here, we identified and characterized the interaction between TopBP1 and the histone demethylase PHF8. We found that PHF8 interacts directly with the BRCT domains 7 + 8 of TopBP1 *via* the PHF8 residue Ser854. Moreover, this interaction was enhanced in the S phase of the cell cycle. More specifically, we asked whether PHF8 is phosphorylated and, if so, which kinases are responsible for the PHF8 phosphorylation, and whether phosphorylation occurs at specific stages of the cell cycle. Our evidence suggests that PHF8 is phosphorylated at Ser854 by the protein kinase CK2 (Figure 7F). This conclusion is supported by three lines of evidence. First, Ser854 forms a consensus site for CK2 kinase. Second, CK2 phosphorylates PHF8 at Ser854 *in vitro* and *in vivo*. Third, the highly specific CK2 kinase inhibitor CX-4945 inhibits CK2-mediated PHF8 phosphorylation at Ser854. Importantly, phosphorylation of PHF8 at Ser854 site was significantly enriched during S phase, which appears to correlate with its interaction with TopBP1. While some studies reported constant CK2 activity during the cell division cycle, there are reports showing that the association of the adenomatous polyposis coli (APC) with CK2 was cell cycle-dependent, with the highest association in G2/M (33), and phosphorylation of eIF5 associated with CK2 only in G1 (34). Moreover, in mitosis, CK2 has been shown to phosphorylate Topoisomerase IIα/β and HDAC1/2 (35,36). These reports suggest a cell cycle-dependent regulation of substrates by CK2. Since CK2 binds to both PHF8 and TopBP1 (Supplemental Figure S8A) and determines PHF8 phosphorylation, we therefore propose that CK2 associates with PHF8 phosphorylation in a cell cycle-dependent manner. Moreover, there is another possibility that CK2 might directly interact with as-yet unidentified factor(s) that regulate the cell cycle-dependent PHF8 phosphorylation. We will work on this possibility to discover the underlying mechanism in future studies.

Our data indicate that depletion of PHF8 led to a decrease in TopBP1 protein level in either normal MCF-10A cell or in breast cancer cells. Treatment with the proteasome inhibitor MG132 largely reversed the decrease in TopBP1 level, which raises the possibility that PHF8 may regulate TopBP1 protein level by preventing its proteasomal degradation. DNA-damage-induced ubiquitination and deubiquitination are major regulators of a number of proteins involved in the DNA-damage response, including TopBP1 and 53BP1 (37,38). It was reported that the E3 ligase UBR5 interacts with TopBP1 (32). Indeed, we found that UBR5 promoted the ubiquitination of TopBP1 and that the E3 ligase activity domain (HECT) of UBR5 is required for UBR5-mediated TopBP1 ubiquitination and degradation. Moreover, PHF8 WT, but not the Ser854A mutant, stabilized TopBP1 protein expression. Together, these results suggest that PHF8 binding to TopBP1 may protect TopBP1 from degradation by UBR5 under normal condition (Figure 7F).

The recovery from replication stress by restarting stalled forks to continue DNA synthesis is crucial for maintaining genome stability. Because loss of TopBP1 or PHF8 impaired DNA replication checkpoint activity, we hypothesized that the increased genome instability in TopBP1- or PHF8-deficient cells could arise from the defective restart of stalled replication forks. Using the DNA fiber assay to monitor replication fork progression under conditions of HU-induced replication stress, we found that restarted forks from TopBP1- or PHF8-deficient cells had significantly shorter CIdU tracts, suggesting that forks in these cells were unable to restart. A similar trend in deficient fork restart was also observed in multiple cultured human cell lines. Thus, it is possible that TopBP1 and PHF8 form a complex, acting under replication stress to promote re-initiation of DNA synthesis at stalled forks.

Taken together, our data provide novel insights into the regulation of protein level and localization of TopBP1 under both normal conditions and replication stress. However, a number of questions arise from our work that will be addressed in future studies. In particular, it remains to be determined how PHF8 and UBR5 would participate in the regulation of TopBP1 protein level. Replication forks that stall after encountering DNA lesions may undergo fork reversal that must be properly protected against degradation of nascent DNA. Whether TopBP1 and PHF8 play a role in replication fork protection is unknown. Because we show that TopBP1 and PHF8 both function in replication fork restart, whether fork restart and fork protection are functionally connected needs further attention.

SUPPLEMENTARY DATA

Supplementary Data are available at NAR Online.

ACKNOWLEDGEMENTS

We would like to thank all our colleagues in the Gong laboratory for insightful discussion and technical assistance. We want to thank Dr Youwei Zhang for valuable suggestions. We thank Dr Cassandra Talerico for critical reading of the manuscript.

Author contributions: Z.G. designed the research; H.F., J.C., A.T., X.S., F.Z., L.L. performed the experiments; O.R., A.A. and Z.G. evaluated data and Z.G. wrote the paper.

FUNDING

National Institutes of Health Grant [R01CA222195 to Z.G., R01CA184137 to A.A.]; Ovarian Cancer Research Fund Alliance Grant [373376, 605161 to Z.G.]; Center of Research Excellence in Gynecologic Cancer (in part); VeloSano Pilot Award. Funding for open access charge: NIH; OCRA.

Conflict of interest statement. None declared.

REFERENCES

1. Cimprich,K.A. and Cortez,D. (2008) ATR: an essential regulator of genome integrity. *Nat. Rev. Mol. Cell Biol.*, **9**, 616–627.
2. Nam,E.A. and Cortez,D. (2011) ATR signalling: more than meeting at the fork. *Biochem. J.*, **436**, 527–536.
3. Sokka,M., Parkkinen,S., Pospiech,H. and Syvaoja,J.E. (2010) Function of TopBP1 in genome stability. *Subcell. Biochem.*, **50**, 119–141.
4. Wardlaw,C.P., Carr,A.M. and Oliver,A.W. (2014) TopBP1: a BRCT-scaffold protein functioning in multiple cellular pathways. *DNA Repair (Amst.)*, **22**, 165–174.
5. Kumagai,A., Lee,J., Yoo,H.Y. and Dunphy,W.G. (2006) TopBP1 activates the ATR-ATRIP complex. *Cell*, **124**, 943–955.
6. Bass,T.E., Luzwick,J.W., Kavanaugh,G., Carroll,C., Dungrawala,H., Glick,G.G., Feldkamp,M.D., Putney,R., Chazin,W.J. and Cortez,D. (2016) ETAA1 acts at stalled replication forks to maintain genome integrity. *Nat. Cell Biol.*, **18**, 1185–1195.
7. Haahr,P., Hoffmann,S., Tollenaere,M.A., Ho,T., Toledo,L.I., Mann,M., Bekker-Jensen,S., Raschle,M. and Mailand,N. (2016) Activation of the ATR kinase by the RPA-binding protein ETAA1. *Nat. Cell Biol.*, **18**, 1196–1207.
8. Lee,Y.C., Zhou,Q., Chen,J. and Yuan,J. (2016) RPA-binding protein ETAA1 is an ATR activator involved in DNA replication stress response. *Curr. Biol.*, **26**, 3257–3268.
9. Delacroix,S., Wagner,J.M., Kobayashi,M., Yamamoto,K. and Karnitz,L.M. (2007) The Rad9-Hus1-Rad1 (9-1-1) clamp activates checkpoint signaling via TopBP1. *Genes Dev.*, **21**, 1472–1477.
10. Lee,J., Kumagai,A. and Dunphy,W.G. (2007) The Rad9-Hus1-Rad1 checkpoint clamp regulates interaction of TopBP1 with ATR. *J. Biol. Chem.*, **282**, 28036–28044.
11. Kumagai,A., Shevchenko,A., Shevchenko,A. and Dunphy,W.G. (2010) Treslin collaborates with TopBP1 in triggering the initiation of DNA replication. *Cell*, **140**, 349–359.
12. Sansam,C.L., Cruz,N.M., Danielian,P.S., Amsterdam,A., Lau,M.L., Hopkins,N. and Lees,J.A. (2010) A vertebrate gene, ticrr, is an essential checkpoint and replication regulator. *Genes Dev.*, **24**, 183–194.
13. Yamane,K., Wu,X. and Chen,J. (2002) A DNA damage-regulated BRCT-containing protein, TopBP1, is required for cell survival. *Mol. Cell. Biol.*, **22**, 555–566.
14. Wang,J., Gong,Z. and Chen,J. (2011) MDC1 collaborates with TopBP1 in DNA replication checkpoint control. *J. Cell Biol.*, **193**, 267–273.
15. Wang,J., Chen,J. and Gong,Z. (2013) TopBP1 controls BLM protein level to maintain genome stability. *Mol. Cell*, **52**, 667–678.
16. Blackford,A.N., Nieminuszczy,J., Schwab,R.A., Galanty,Y., Jackson,S.P. and Niedzwiedz,W. (2015) TopBP1 interacts with BLM to maintain genome stability but is dispensable for preventing BLM degradation. *Mol. Cell*, **57**, 1133–1141.
17. Sun,L., Huang,Y., Edwards,R.A., Yang,S., Blackford,A.N., Niedzwiedz,W. and Glover,J.N.M. (2017) Structural insight into BLM recognition by TopBP1. *Structure*, **25**, 1582–1588.
18. Gong,Z., Kim,J.E., Leung,C.C., Glover,J.N. and Chen,J. (2010) BACH1/FANCJ acts with TopBP1 and participates early in DNA replication checkpoint control. *Mol. Cell*, **37**, 438–446.
19. Liu,S., Shiotani,B., Lahiri,M., Marechal,A., Tse,A., Leung,C.C., Glover,J.N., Yang,X.H. and Zou,L. (2011) ATR autophosphorylation as a molecular switch for checkpoint activation. *Mol. Cell*, **43**, 192–202.
20. Feng,W., Yonezawa,M., Ye,J., Jenuwein,T. and Grummt,I. (2010) PHF8 activates transcription of rRNA genes through H3K4me3 binding and H3K9me1/2 demethylation. *Nat. Struct. Mol. Biol.*, **17**, 445–450.
21. Kleine-Kohlbrecher,D., Christensen,J., Vandamme,J., Abarrategui,I., Bak,M., Tommerup,N., Shi,X., Gozani,O., Rappsilber,J., Salcini,A.E. *et al.* (2010) A functional link between the histone demethylase PHF8 and the transcription factor ZNF711 in X-linked mental retardation. *Mol. Cell*, **38**, 165–178.
22. Liu,W., Tanasa,B., Tyurina,O.V., Zhou,T.Y., Gassmann,R., Liu,W.T., Ohgi,K.A., Benner,C., Garcia-Bassets,I., Aggarwal,A.K. *et al.* (2010) PHF8 mediates histone H4 lysine 20 demethylation events involved in cell cycle progression. *Nature*, **466**, 508–512.
23. Qi,H.H., Sarkissian,M., Hu,G.Q., Wang,Z., Bhattacharjee,A., Gordon,D.B., Gonzales,M., Lan,F., Ongusaha,P.P., Huarte,M. *et al.* (2010) Histone H4K20/H3K9 demethylase PHF8 regulates zebrafish brain and craniofacial development. *Nature*, **466**, 503–507.
24. Lee,Y., Katyal,S., Downing,S.M., Zhao,J., Russell,H.R. and McKinnon,P.J. (2012) Neurogenesis requires TopBP1 to prevent catastrophic replicative DNA damage in early progenitors. *Nat. Neurosci.*, **15**, 819–826.
25. Mendez,J. and Stillman,B. (2000) Chromatin association of human origin recognition complex, cdc6, and minichromosome maintenance proteins during the cell cycle: assembly of prereplication complexes in late mitosis. *Mol. Cell. Biol.*, **20**, 8602–8612.
26. Schwab,R.A. and Niedzwiedz,W. (2011)Visualization of DNA replication in the vertebrate model system DT40 using the DNA fiber technique. *J. Vis. Exp.*, **56**, e3255.
27. Quinet,A., Carvajal-Maldonado,D., Lemacon,D. and Vindigni,A. (2017) DNA fiber analysis: mind the gap!*Methods Enzymol.*, **591**, 55–82.
28. Chowdhury,P., Lin,G.E., Liu,K., Song,Y., Lin,F.T. and Lin,W.C. (2014) Targeting TopBP1 at a convergent point of multiple oncogenic pathways for cancer therapy. *Nat. Commun.*, **5**, 5476.
29. Leung,C.C., Gong,Z., Chen,J. and Glover,J.N. (2011) Molecular basis of BACH1/FANCJ recognition by TopBP1 in DNA replication checkpoint control. *J. Biol. Chem.*, **286**, 4292–4301.
30. Manke,I.A., Lowery,D.M., Nguyen,A. and Yaffe,M.B. (2003) BRCT repeats as phosphopeptide-binding modules involved in protein targeting. *Science*, **302**, 636–639.
31. Yu,X., Chini,C.C., He,M., Mer,G. and Chen,J. (2003) The BRCT domain is a phospho-protein binding domain. *Science*, **302**, 639–642.
32. Honda,Y., Tojo,M., Matsuzaki,K., Anan,T., Matsumoto,M., Ando,M., Saya,H. and Nakao,M. (2002) Cooperation of HECT-domain ubiquitin ligase hHYD and DNA topoisomerase II-binding protein for DNA damage response. *J. Biol. Chem.*, **277**, 3599–3605.
33. Homma,M.K., Li,D., Krebs,E.G., Yuasa,Y. and Homma,Y. (2002) Association and regulation of casein kinase 2 activity by adenomatous polyposis coli protein. *PNAS*, **99**, 5959–5964.
34. Homma,M.K., Wada,I., Suzuki,T., Yamaki,J., Krebs,E.G. and Homma,Y. (2005) CK2 phosphorylation of eukaryotic translation initiation factor 5 potentiates cell cycle progression. *PNAS*, **102**, 15688–15693.
35. Daum,J.R. and Gorbsky,G.J. (1998) Casein kinase II catalyzes a mitotic phosphorylation on threonine 1342 of human DNA topoisomerase IIalpha, which is recognized by the 3F3/2 phosphoepitope antibody. *J. Biol. Chem.*, **273**, 30622–30629.
36. Khan,D.H., He,S., Yu,J., Winter,S., Cao,W., Seiser,C. and Davie,J.R. (2013) Protein kinase CK2 regulates the dimerization of histone deacetylase 1 (HDAC1) and HDAC2 during mitosis. *J. Biol. Chem.*, **288**, 16518–16528.
37. Xu,Z.X., Timanova-Atanasova,A., Zhao,R.X. and Chang,K.S. (2003) PML colocalizes with and stabilizes the DNA damage response protein TopBP1. *Mol. Cell. Biol.*, **23**, 4247–4256.
38. Zhang,D., Zaugg,K., Mak,T.W. and Elledge,S.J. (2006) A role for the deubiquitinating enzyme USP28 in control of the DNA-damage response. *Cell*, **126**, 529–542.